ASEG2024
HOBART

GSWA petrophysics update: insights from physical property cross plots

Sasha Banaszczyk
Department of Energy, Mines, Industry Regulation and Safety
Geological Survey of Western Australia
sasha.banaszczyk@demirs.wa.gov.au

SUMMARY

GSWA commenced a five-year petrophysical sampling program in 2021. The data collected as part of this program will enable more informed decision making for the resources exploration industry, government agencies and solid Earth science research in WA. To date, 171 publicly available drillcores have been petrophysically sampled from across WA. We present this data and complete a first-pass regional-scale analysis of the magnetic susceptibility, galvanic resistivity, dry bulk density, chargeability, p-wave velocity, and apparent porosity for a variety of rock types. This first pass analysis compared different rock types from different regions, however, further interrogation of the data on a more local scale will improve our understanding of the physical property trends for different alteration assemblages, mineralisation styles, and lithologies for different geographical regions. All petrophysical data results are published to GSWA's MAGIX platform and can be downloaded by searching for the petrophysics method.

Key words: petrophysics, physical properties, Western Australia, geology

INTRODUCTION

The Geological Survey of Western Australia (GSWA) has a five-year program facilitated through the Western Australian Government's Exploration Incentive Scheme (EIS) to collect petrophysical data from EIS co-funded drillcore, GSWA stratigraphic drillcore, or company-held core on request from GSWA. The tender for data acquisition was awarded to Terra Petrophysics at project commencement in 2021. The long-term objective of the program is to acquire a broad suite of data to define the petrophysical characteristics of key lithostratigraphic units, alteration patterns or major mineral system environments. It is anticipated that 1000–2000 samples will be analysed annually. Petrophysical cores are primarily chosen where data can assist in the modelling of geophysical data in regions with cover, the interpretation of recent or upcoming 2D seismic lines, and the classification of regional stratigraphy (often in conjunction with geochemistry). Selected core samples are analysed for the following petrophysical properties:

- induced polarization (chargeability) and galvanic resistivity
- inductive conductivity
- magnetic susceptibility
- remanent magnetization
- dry bulk density
- apparent porosity
- P-wave sonic velocity
- spectral radiometrics

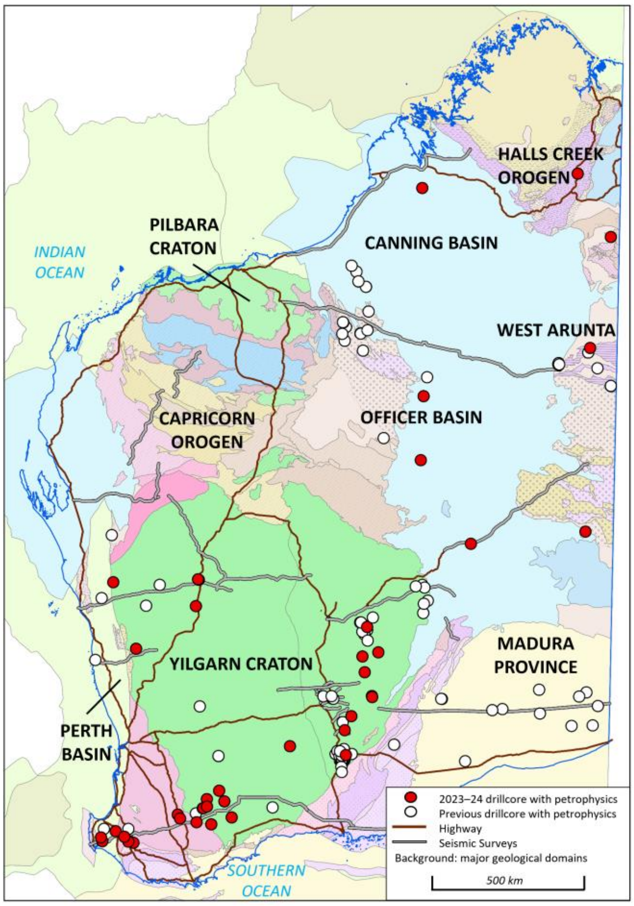

Figure 1. Location map of GSWA drill hole locations where petrophysical data has been collected. Red points show the locations of drillcores sampled for petrophysics over 2023–24.

To date, 8,622 samples have been analysed for petrophysical properties from a total of 171 publicly available drillcores located across WA (Figure 1). Data collected over 2023–24 include 1701 samples from 40 publicly available drillcores from the Officer, Canning, and Perth Basins, Tanami, West Arunta, and Kalgoorlie regions, Halls Creek Orogen, and the South West Yilgarn and Youanmi Terranes (Figure 1). Here we present a summary of all GSWA physical property measurements from across WA.

DATA OVERVIEW

The cross plots in Figure 2 display a total of 6898 samples. Visible metal sulphides, oxides, and other natural metal minerals (termed 'mineralisation') were logged in a small proportion of samples (n=1435) and thus were excluded from further analysis, and 289 samples missing p-wave velocity data were also removed. Minimum logging requirements are: 1. rock type, and 2. lithology information, therefore, where petrophysical sampling has occurred as a supplement to other projects (e.g., geochemistry or geochronology specific), information such as alteration or mineralisation may not always be captured. Therefore, it is sensible to start data analysis with simplified unmineralized rock groupings before further interrogating individual logging comments which may or may not contain alteration or mineralisation information. The logged geology was simplified to 24 rock groupings based on GSWA rock and lithology types to facilitate general conclusions of the (large) petrophysical dataset. It is recognised that a more complete understanding of petrophysical property trends will be gained with future work aimed at discriminating alteration and mineralisation for local geological domains, especially where coincident geochemistry or spectral data are available (Dentith, Adams, and Bourne, 2018).

PHYSICAL PROPERTIES

The first pass petrophysical data analysis looked at the following physical properties: magnetic susceptibility, dry bulk density, galvanic resistivity, chargeability, p-wave velocity, and apparent porosity. Here we present a brief overview of these properties.

Magnetic susceptibility is a measure of a materials ability to become magnetised in the presence of an external magnetic field (Lapointe, Morris, and Harding, 1986) and is controlled by the percentage composition of ferromagnetic minerals such as magnetite, pyrrhotite, maghemite, and pentlandite and to a lesser extent, antiferromagnetic minerals such as hematite and paramagnetic minerals such as ilmenite (Rauen, Soffel, and Winter, 2000; Rosenblum and Brownfield, 1999; Abrajevitch et al., 2021). Mafic and ultramafic lithologies are more magnetically susceptible than felsic and sedimentary lithologies as they are typically more abundant in magnetic minerals (Dentith et al., 2020).

Density, and velocity measurements are largely controlled by bulk rock properties including mineral composition and rock porosity (i.e., pore spaces between grains and bulk rock fractures and microfractures). Dry bulk density is the ratio of dry rock mass to the total rock volume (Emerson, 1990), and porosity is the ratio of void volume to total rock volume determined from water saturated weights, dry weights, and the buoyancy-determined volume of a sample (Julianti et al., 2022). P-wave velocities can be used to understand the acoustic impedance of a rock and typically increases with density and decreases with porosity because it is dependent on a rock's resistance to bulk compression, its rigidity, and its density (Adams, 2020, and references therein).

Electrical resistivity is a measure of a materials ability to allow the flow of an electrical current. Resistivity is linked to different rock features including mineral composition and the interconnectivity of certain mineral species as well as a rocks texture or the presence of fractures (Banaszczyk, 2020, and references therein). Common electrically conductive minerals include metal sulphides, graphite, and clays. Where conductive mineral species are interconnected, the resistivity of a rock sample will decrease, however, where conductive minerals are disseminated, the resistivity can increase. In contrast, chargeability is a measure of a rocks ability to store and release an electrical charge after an applied current has been turned off (Revil et al., 2018; Dentith and Mudge, 2014). Therefore, where metal sulphides, clays, and fibrous minerals are less connected and more disseminated, the chargeability can increase (Dentith and Mudge, 2014). Porosity and permeability, and the size and shape of mineral grains also impact the chargeability of a rock sample (Dentith and Mudge, 2014; Fitzpatrick, 2006).

DATA OVERVIEW

In Figure 2(a) magnetic susceptibility is plotted against resistivity. Unsurprisingly, the felsic (pink colour) and sedimentary siliciclastic units (open yellow squares) are the least magnetically susceptible (below the red line), while mafic and ultramafic units (blue and purple colours) have the largest magnetic susceptibilities (mostly plotting above the red trend line). From the felsic unit, the most magnetically susceptible samples are the syenogranites which may contain non-visible accessory magnetite contributing to their large magnetic susceptibilities. The most magnetically susceptible and conductive carbonatite samples (dark pink points) are from the deepest core samples through the Mount Weld Carbonatite suggesting these samples may contain magnetite not identified in the logging. The black shale material and graphite which comprises the Kapia Slate of the Kalgoorlie Terrane makes it the most conductive lithology of the sedimentary siliciclastic shale unit (open blue squares), while bedded and massive sandstones are the most conductive samples of the sedimentary siliciclastic unit (open yellow squares) due to their high porosity (and moisture content). BIF (dark blue triangle) samples have large magnetic susceptibilities and resistivities due to their magnetite and resistive Fe-silicate and -carbonate content, while regolith (orange triangles) samples are conductive and have a broad range of low magnetic susceptibilities due to their high percentage composition of clay and silicate minerals.

Figure 2(b) compares magnetic susceptibility against density. As expected, sedimentary siliciclastic units (open yellow squares) and regolith samples (orange triangles) plot in a quadrant of low magnetic susceptibility and low density. In contrast the felsic lithologies (pink colour) and metasedimentary siliciclastic units (yellow squares) cluster within a discrete zone of densities between ~2.5-2.8 g/cm^3 (left of the red line). While the mafic units (blue colour) have a broad range of magnetic susceptibilities and a broad range of high densities (right of the red line), the densest values form the mafic units are associated with meta-dolerite, meta-gabbro, and mafic granulite samples. The densest ultramafic lithologies (purple points) are komatiites, and the lowest density ultramafic lithologies are lamprophyre samples, which in contrast to the komatiites, comprise a high percentage of micas and amphiboles that lower their density. Interestingly, the ultramafic units with low magnetic susceptibilities tend to be associated with samples collected on core from the Kalgoorlie Terrane while more magnetically susceptible ultramafic samples come from the Kurnalpi Terrane. As expected, the BIF samples are the densest and most magnetically susceptible rock type.

A broad range of resistivities and chargeabilities exists across all rock types in Figure 2(c) which includes a broad cluster of highly chargeable and conductive values (red circle) consistent with weathered regolith samples containing clay minerals (orange triangles), sedimentary siliciclastic units (open yellow squares) with high porosity, and graphitic rich sedimentary siliciclastic shales (open blue squares). Carbonatite (pink points) and ultramafic units (purple colours) form a moderately conductive cluster over a broad range of moderate to low chargeabilities (black circle). This cluster supports the assumption made from Figure 2(a) that some non-visible magnetite may exist in these samples. In contrast, mafic units (blue colour) have the broadest range of chargeabilities, with the most chargeable mafic units including dolerites, gabbros, basalts, and their deformed equivalents, as well as amphibolites and mafic granulites. In contrast, felsic rocks (pink colours) cluster at low chargeabilities over a broad range of resistivities located to the left of the red trend line, consistent with large grain sizes, fewer fibrous mineral components, and/or a lack of non-visible disseminated mineralisation in these samples.

Typically, p-wave velocities of silicate rocks increase with density where they are more mafic and/or increase in metamorphic grade (Salisbury, Harvey, and Matthews, 2003). Additionally, fractures and microfractures significantly impact p-wave velocities measured on drillcore (Adams, 2020). In Figure 2(d) it is unsurprising that the felsic (pink colours) and sedimentary units (yellow colours) have slightly lower p-wave velocities and densities than mafic (blue colours) units (see clusters either side of the red trend line), and that the lowest densities and p-wave velocities (Figure 2(d)-black circle) are from massive sandstone samples within the sedimentary siliciclastic group (open yellow squares). The metasedimentary units (yellow squares) have slightly higher p-wave velocities than felsic units which is consistent with their logged silica and/or felspar alteration, while the lower velocity measurements seen within the felsic group are consistent with chlorite and biotite altered samples. The cherts (green triangles) have high silica content and low porosities which is consistent with their high p-wave velocities across a range of high-densities.

Figure 2(d) compares apparent porosity against density with common mineral trends following Emerson and Yang, (1997). The sedimentary siliciclastic lithologies (yellow open squares) are partially clustered around dolomitic and quartz/feldspar trends which is consistent with their logged lithologies and alteration. These units also have a wide range of porosities at lower densities where samples are dominated by massive sandstones. Rare mafic and ultramafic samples (blue and purple colours, respectively) lie on the low-density side of trend line 3 which may indicate that they are weathered to partially weathered, but elsewhere, mafic samples have a wide range of densities on the right side of trend line 2 which is consistent with their logged alteration assemblages including: amphibole, chlorite, biotite, carbonate, and minor quartz/silica alteration. As expected, ultramafic clusters are located between trend lines 2 to 4 consistent with serpentine and talc alteration in these samples, and carbonatite samples (dark pink points) cluster around the dolomite trend line.

CONCLUSIONS

Petrophysical measurements and geological logging alone can be used to make meaningful conclusions about physical property trends, even when limited geological information and metrics including percentage sulphide mineralisation or alteration are unavailable. For example, some logging discrepancies have been identified where magnetite may be present in carbonatite and ultramafic samples because these rocks exhibit high magnetic susceptibilities, and moderately conductivities and chargeabilities. Separately, high porosities and low densities of some mafic and ultramafic units can be explained if these samples are partially weathered or fractured. Future work will further interrogate measured physical properties with respect to different alteration assemblages, mineralisation, and weathering for different geological terranes and aim to integrate available geochemistry and spectral data.

REFERENCES

Abrajevitch, A., A. P. Roberts, B. J. Pillans, and R. S. Hori, 2021, Unexpected magnetic behaviour of natural hematite-bearing rocks at low temperatures: Geochemistry, Geophysics, Geosystems, **22,** http://dx.doi.org/ 10.1029/2021GC010094.

Adams, C., 2020, Integrating petrophysical, lithogeochemical, and mineralogical data to understand the physical properties of altered mafic and ultramafic rocks: implications for geophysical exploration: Doctor of Philosophy, The University of Western Australia, http://dx.doi.org/ 10.26182/xg61-fa34.

Banaszczyk, S., 2020, Extracting reliable geological information from electromagnetic datasets in a regolith dominated terrain: Capricorn Orogen, Western Australia: Doctor of Philosophy, The University of Western Australia, http://dx.doi.org/ 10.26182/5eabb885884db.

Dentith, M., C. Adams, and B. Bourne, 2018, The use of petrophysical data in mineral exploration: A perspective: ASEG Extended Abstracts, **2018**, 1–4, http://dx.doi.org/ 10.1071/ASEG2018abW9_1F.

Dentith, M., R. J. Enkin, W. Morris, C. Adams, and B. Bourne, 2020, Petrophysics and mineral exploration: a workflow for data analysis and a new interpretation framework: Geophysical Prospecting, **68**, 178–99, http://dx.doi.org/ 10.1111/1365-2478.12882.

Dentith, M. C., and S. T. Mudge, 2014, Geophysics for the mineral exploration geoscientist: Cambridge University Press.

Emerson, D. W., 1990, Notes on mass properties of rock-density, porosity, permeability: Exploration Geophysics, **21**, 209–16.

Emerson, D. W., and Y. P. Yang, eds., 1997, Insights from laboratory mass property crossplots Special issue, *Preview*, no. 70. Accessed 10 July 2024, https://www.aseg.org.au/sites/default/files/PVv1997n070.pdf.

Fitzpatrick, A. D., 2006, Scale dependent electrical properties of sulphide deposits: Doctor of Philosophy, University of Tasmania, http://dx.doi.org/ 10.25959/23210849.v1.

Julianti, D., Fatkhan, E. Dinanto, and A. S. Murtani, eds., 2022, Petrophysics analysis for determination of density porosity and neutron-density porosity on carbonate rock in East Java Basin: IOP Publishing, http://dx.doi.org/ 10.1088/1755-1315/1031/1/012023.

Lapointe, P., W. A. Morris, and K. L. Harding, 1986, Interpretation of magnetic susceptibility: a new approach to geophysical evaluation of the degree of rock alteration: Canadian Journal of Earth Sciences, **23**, 393–401, http://dx.doi.org/ 10.1139/e86-041.

Rauen, A., H. C. Soffel, and H. Winter, 2000, Statistical analysis and origin of the magnetic susceptibility of drill cuttings from the 9.1-km-deep KTB drill hole: Geophysical Journal International, **142**, 83–94, http://dx.doi.org/ 10.1046/j.1365-246x.2000.00141.x.

Revil, A., T. Tartrat, F. Abdulsamad, A. Ghorbani, and A. Coperey, 2018, Chargeability of porous rocks with or without metallic particles: Petrophysics – The SPWLA Journal of Formation Evaluation and Reservoir Description, **59**, 544–53, http://dx.doi.org/ 10.30632/PJV59V4-2018a8.

Rosenblum, S., and I. K. Brownfield, 1999, Magnetic susceptibility of minerals, https://pubs.usgs.gov/of/1999/ofr-99-0529/MAGRPTfinal.pdf. Accessed 05 July 2024.

Salisbury, M. H., C. W. Harvey, and L. Matthews, 2003, 1. The Acoustic properties of ores and host Rocks in hardrock terranes, *in* D. W. Eaton, B. Milkereit, and M. H. Salisbury, eds., Hardrock seismic exploration: Society of Exploration Geophysicists, 9–19, http://dx.doi.org/ 10.1190/1.9781560802396.ch1.

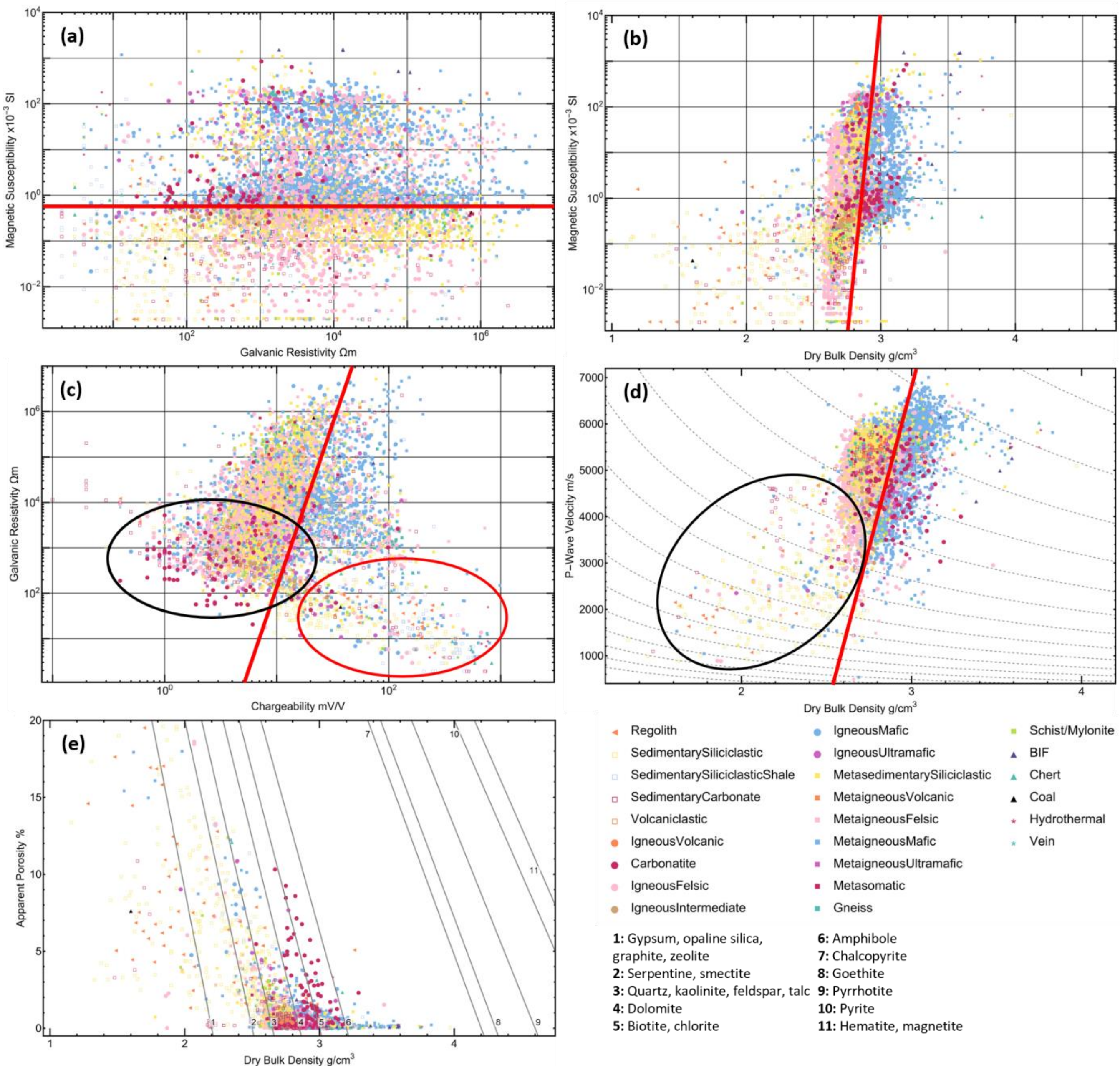

Figure 2. Cross plots of (a) magnetic susceptibility against galvanic resistivity, (b) magnetic susceptibility against dry bulk density, (c) galvanic resistivity against chargeability, (d) p-wave velocity against dry bulk density with lines of acoustic impedance with a reflection coefficient equal to 0.06 from Salisbury, Harvey, and Matthews, (2003), and (e) apparent porosity against dry bulk density with mineral trends lines from Emerson and Yang, (1997). See text for descriptions of annotated circles and lines.